Partial Discharge Localization in Power Transformers Using Invariant Extended Kalman Filter

Wasim Al-Masri, Ali Wadi, *Member, IEEE*, Mamoun F. Abdel-Hafez, *Senior Member, IEEE*, Hashim A. Hashim, *Senior Member, IEEE*, and Ayman H. El-Hag, *Senior Member, IEEE*

Abstract— This article proposes a novel invariant extended Kalman filter (IEKF), a recently modified version of the extended Kalman filter (EKF), to estimate partial discharge (PD) location in a transformer insulation system model. An acoustic signal measurement is utilized to localize the PD location. Unlike conventional EKF methods, where the correction term used to update the state is linearly proportional to the output error, the correction term of the proposed algorithm is independent of the output error, resulting in a fast response with a significant reduction in the estimation error. In contrast to the EKF, the proposed method can successfully mimic the nonlinear dynamics and mitigate measurement noise stochasticity. Moreover, even if the measurement model fails to fully capture the PD's dynamics, the IEKF will still sustain a reasonable performance. In contrast, conventional EKFs can easily diverge if a mismatch between the measurement model and the true measurement occurs. Experimental results are shown to verify the proposed method's performance compared to a recently published variant of the EKF.

Index Terms— Acoustic emission (AE) sensors, extended Kalman filter (EKF), invariant extended Kalman filter (IEKF), localization, partial discharge (PD), transformer oil/paper insulation system.

I. Introduction

THE integrity of the power grid depends on the health conditions of different power system components such as transformers, circuit breakers, and underground cables. One of the leading causes of power system components failure is the initiation of partial discharge (PD) that eventually leads to the complete failure of the insulation system [1]. PD can be initiated at different locations inside the transformer tank leading to the gradual aging of transformer oil and cellulose paper and eventually to the transformer's complete

Wasim Al-Masri, Ali Wadi, and Mamoun F. Abdel-Hafez are with the Department of Mechanical Engineering, American University of Sharjah, Sharjah, United Arab Emirates (e-mail: walmasri@aus.edu; awadi@aus.edu; mabdelhafez@aus.edu).

Hashim A. Hashim is with the Department of Mechanical and Aerospace Engineering, Carleton University, Ottawa, ON K1S 5B6, Canada (e-mail: hhashim@carleton.ca).

Ayman H. El-Hag is with the Department of Electrical Engineering, University of Waterloo, Waterloo, ON N2L 3G1, Canada (e-mail: ahalhaj@uwaterloo.ca).

failure. Therefore, monitoring and localizing the PD activities inside power transformers act as preventive maintenance that minimizes the risk of sudden transformer failure.

The release of the PD energy can generate electromagnetic and ultrasonic waves. As a result, various sensors, such as radio frequency (RF) antennas, high-frequency current transformers (HFCTs), and acoustic emission (AE) sensors, can be employed to detect the PD [1]. HFCT can be utilized to detect PD activities but has several disadvantages that limit its field application. For example, HFCT suffers from a low signal-to-noise ratio, limited access to the ground wire, and cannot be used to localize the PD source. On the other hand, an RF antenna can be used to detect and localize the PD locations if multiple antennas are utilized. However, unless these antennas are preinstalled inside the transformer tank during the manufacturing stage, this approach is not practical because it is intrusive. Furthermore, the RF antenna is susceptible to electromagnetic noise and requires a relatively expensive data acquisition system due to the need for a high sampling rate. Alternatively, AE measurement systems are relatively cost-effective and nonintrusive and can be used to localize PD sources. Furthermore, PD localization (PDL) employing the AE technique is commonly done by estimating the time difference of arrival (TDOA) between signals captured at multiple acoustic sensors placed on the walls of the transformer tank. However, AE sensors suffer from noise that may hinder their applicability in the field.

Hence, AE PD signal denoising is commonly used prior to any PDL and/or classification [2], [3]. However, one of the main limitations of denoising techniques for AE PD signals is the need to estimate the environmental acoustic noise, which may not be accessible. The authors used the source-filter model in [4] to estimate the excitation source and isolate it from the physical system's acoustic response. This PD pulse estimation can help precisely calculate the TDOA and, thus, the PD position, alleviating the necessity for PD denoising. The deformation of the PD shape, on the other hand, could be caused by factors other than noise, such as oil temperature and barriers between the PD source and the sensor.

A pattern recognition-based method for PDL in an oil-filled transformer using acoustic measurements was presented as an alternative [5]. The method works by dividing the transformer tank into smaller zones. The zone with the smallest spatial

distance between its standard pattern vector and its indeterminate pattern vector could reveal the PD location by comparing the spatial distance between the two pattern vectors. The size of the selected zones affects the proposed model's reliability. Minimizing the selected zones increases the accuracy but increases the computational complexity.

In any measurement system, there are two types of propagation errors: systematic and random. The primary goal of our study is to determine the arrival time of various acoustic signals. Systematic and random faults influencing the sensor measurement include bias in the acoustic sensor readings and external acoustic noise. The authors used different estimation strategies to localize the PD source using a transformer insulation model in earlier works [6], [7], [8], [9]. In [6], we suggested a nonlinear sequential technique to detect bias in acoustic sensor readings to improve the accuracy of PDL. By progressively processing the measurements of the acoustic sensors, the suggested approach finds the malfunctioning sensor and determines the bias error integrated into its measurements. The estimator can still benefit from utilizing the sensor's measurements to detect the PD's location by subtracting the discovered bias from the related sensor's measurements. Both an extended Kalman filter (EKF) and a multiple-model adaptive EKF (AEKF) were suggested in [7] to estimate the ideal PD location in the transformer insulation system after identifying and reducing the bias associated with a malfunctioning sensor. The suggested method is used to probabilistically determine the noise covariance of AE signals, resulting in an optimal PD location estimate. In [8], more work was done to use a maximum likelihood estimation (MLE) approach to discover the statistics of the dynamics and measurement noise sequences and to use that information to improve PD location predictions. A variety of estimation algorithms were described in [9] to estimate the PD location that considers both measurement and dynamics noise uncertainty as well as PD model uncertainty. The EKF, the unscented Kalman filter (UKF), the smooth variable structure filter (SVSF), the EK-SVSF, and the UK-SVSF are among the estimators utilized. The results showed that the UK-SVSF filter has the best estimation performance.

A. Contributions

This article proposes a novel invariant EKF (IEKF) for estimating the PD location in an oil insulation system. The proposed method enhances the estimation performance of the PD's location, as verified experimentally in this article. Unlike the conventional EKF, the IEKF mimics the system's nonlinearity through the propagation and measurement update steps, significantly enhancing the estimation's performance. The invariance property allows the IEKF to preserve the model's geometry, preventing the error from divergence. Therefore, in comparison with the EKF, the IEKF produces better tracking performance. The IEKF is presented discretely to facilitate the implementation process at a low sampling rate. As shown through the experimental verification, the IEKF outperforms the EKF and UK-SVSF in the presence of a significant mismatch between the model output and the true measurement. The difference between the filters becomes more
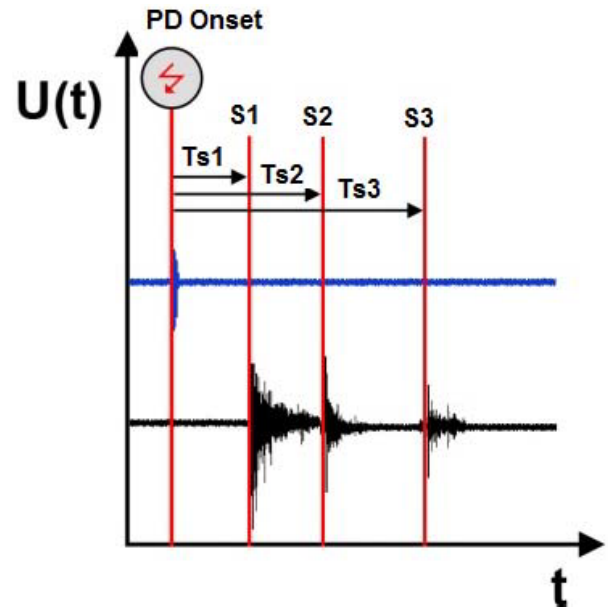

Fig. 1.   Schematic drawing of PD initialization to the sensors.

apparent when the initial state estimate is far from the true state.

B. Structure

The rest of this article is organized as follows. Section II demonstrates the method proposed in this work. The experimental setup and results are discussed in Section III. Finally, Section IV gives concluding remarks.

C. Notation

Throughout this article, $\mathbb{R}$ stands for the set of real numbers, $\mathbb{R}^{n \times m}$ defines an $n \times m$ real dimensional space, and $\mathbb{Z} = \{0, 1, 2, \ldots\}$ is the set of nonnegative integer numbers. $\mathbf{I}_n \in \mathbb{R}^{n \times n}$ stands for an $n \times n$ identity matrix. For any $x_t \in \mathbb{R}^n$ and $t \in \mathbb{Z}$, x_t refers to the value of x at sample instant t. $\exp(\cdot)$, $\mathbb{P}(\cdot)$, $\mathbb{E}[\cdot]$, $\text{sign}(\cdot)$, and $\text{diag}(\cdot)$ represent the exponential, probability, expected value, sign, and diagonal of a component, respectively.

II. METHODOLOGY

A. Problem Formulation

The PD system model used was presented in [6]. In this model, the absolute time measurements are shown in Fig. 1. These time measurements are modeled in (1) as a function of the two unknown PD coordinates in space (x, y), the measured arrival times T_{si}, the assumed sound velocity v_S, and the Cartesian sensor coordinates (x_{si}, y_{si})

$$(x - x_{si})^2 + (y - y_{si})^2 = (v_S T_{si})^2. \tag{1}$$

Fig. 2(a) shows the placement of the AE sensors around the transformer tank. The PD source can be experimentally initiated in any of the circled positions, as shown in Fig. 2(b).
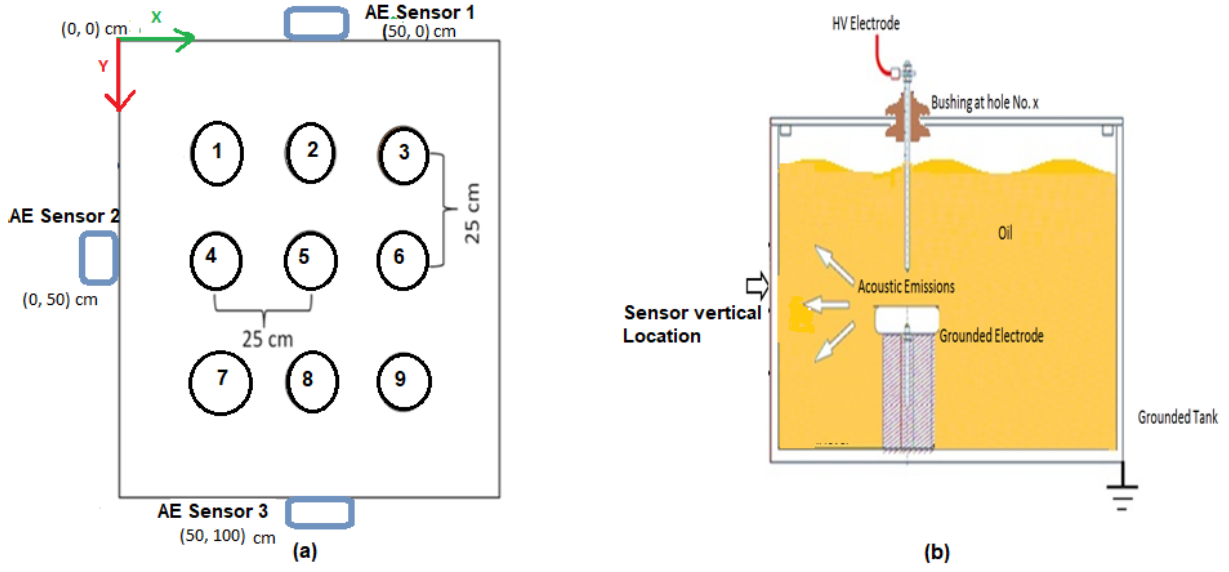
Fig. 2. PD initialization and modeling: (a) top view (b) side view.

The measurements of the sensors can be put in an equation form as

$$y_t = h(x_{p,t}, x_s) + v_t + \mu_t \qquad (2)$$

$$h(x_{p,t}, x_s) = \begin{bmatrix} \sqrt{(x_t - x_{s1})^2 + (y_t - y_{s1})^2} \\ \sqrt{(x_t - x_{s2})^2 + (y_t - y_{s2})^2} \\ \sqrt{(x_t - x_{s3})^2 + (y_t - y_{s3})^2} \end{bmatrix} \qquad (3)$$

where y_t is the vector of the sensors' measurements, $x_{p,t}$ is the PD's position vector with respect to the origin, x_s is the sensors' position vector, h is a vector of the relation between the PD's position and the sensors' positions, v_t is the vector of the sensors' measurements' noise vector of zero mean and covariance R_t, and μ_t is the vector of possible sensors' measurements bias. This bias term is assumed to have been estimated and removed using the method proposed in [6]. In addition, (x_t, y_t) are the x_t and y_t components of $x_{p,t}$, respectively, and (x_{si}, y_{si}) are the x and y components of sensor i's position, respectively. The discretized dynamic equation of the system is given as follows:

$$x_{p,t} = F x_{p,t-1} + \omega_{t-1} \qquad (4)$$

where F is the transition matrix and is defined as a 2×2 identity matrix and ω_t is the Gaussian white dynamics noise with zero mean and covariance Q_t.

B. Overview of EKF

The EKF, using a set of observations, evaluates in real time the updated estimate denoted by $\hat{x}_{p,t} = \hat{x}_{p,t|t} \in \mathbb{R}^2$, which represents the state estimate utilizing all the measurements up to time t. For a linear system, this represents an unbiased estimate of the state. In addition, the EKF determines the accuracy measure $\mathbb{P}(x_{p,t}|y_{1:t})$ of the estimated state, where $y_{1:t}$ is the sequence of observations $y_1, y_2, \ldots, y_t$. The filter operates in two stages: propagation and measurement update. In the propagation stage, $\hat{x}_{p,t-1} = \hat{x}_{p,t-1|t-1}$ is defined

utilizing the observed y_{t-1} and is propagated deterministically mimicking the nonlinearity in (4) such that

$$\hat{x}_{p,t|t-1} = F \hat{x}_{p,t-1}. \qquad (5)$$

Let us define the error between the true and the estimated state as

$$\begin{cases} e_{t-1} = x_{p,t-1} - \hat{x}_{p,t-1} \\ e_{t|t-1} = x_{p,t} - \hat{x}_{p,t|t-1} \end{cases} \qquad (6)$$

where subscript $t-1$ is related to a priori state employed during propagation, while the subscript $t|t-1$ is utilized during the measurement update or the correction step. Hence, the covariances associated with the estimation error are defined by $P_{t-1} = \mathbb{E}[e_{t-1}e_{t-1}^\top] \in \mathbb{R}^{2\times2}$, $P_{t|t-1} = \mathbb{E}[e_{t|t-1}e_{t|t-1}^\top]$, and $P_t = \mathbb{E}[e_t e_t^\top]$. The EKF operates based on the system's model linearization performed using the first-order Taylor series expansion of the nonlinear functions $h(\cdot, \cdot)$ described in (3) where

$$\begin{cases} e_{t|t-1} = F e_{t-1} + \omega_t \\ y_t - h(\hat{x}_{p,t|t-1}) \approx H_t e_{t|t-1} + v_t \end{cases} \qquad (7)$$

where $H_t = (\partial h(\hat{x}_{p,t|t-1}, 0))/\partial x_p$, and the high-order terms have been disregarded, visit [10]. P_{t-1} is propagated using the linearized system's error dynamics in (7) as

$$P_{t|t-1} = F_t P_{t-1} F^\top + Q_t. \qquad (8)$$

In the measurement update stage, an innovation component is defined as $z_t = y_t - h(\hat{x}_{p,t|t-1})$. The measurement and covariance updates are defined by

$$\hat{x}_{p,t} = \hat{x}_{p,t|t-1} + K_t z_t \qquad (9)$$

$$P_t = (\mathbf{I}_n - K_t H_t) P_{t|t-1}. \qquad (10)$$

Algorithm 1 summarizes the implementation steps of EKF.

Algorithm 1 EKF Implementation Steps

Initialization:

1: Set $\hat{x}_{p,0} \in \mathbb{R}^2$, and the covariance $\hat{P}_0 \in \mathbb{R}^{2 \times 2}$

loop

2: Define H_t, as in (7).

3: From (2) & (4), define $Q_t = \text{Cov}(\omega_t)$ and $R_t = \text{Cov}(v_t)$.
   /* Propagation */

4: $\hat{x}_{p,t|t-1} = F \, \hat{x}_{p,t-1}$

5: $P_{t|t-1} = F_t P_{t-1} F_t^\top + Q_t$
   /* Measurement update */

6: $S_t = H_t P_{t|t-1} H_t^\top + R_t$

7: $K_t = P_{t|t-1} H_t^\top S_t^{-1}$

8: $z_t = y_t - h(\hat{x}_{p,t|t-1})$

9: $\hat{x}_{p,t} = \hat{x}_{p,t|t-1} + K_t z_t$

10: $P_t = (\mathbf{I}_n - K_t H_t) P_{t|t-1}$

end loop

C. UK-SVSF

The SVSF is paired with the UKF to achieve a noise-optimal and model-robust estimator, as discussed in [9]. The SVSF method is proposed to improve the filter's resistance to modeling uncertainty and the estimated state's smoothness. On the other hand, SVSF does not optimize the estimated state against dynamics and measurement noise sequences, affecting estimation accuracy. The SVSF is paired with the UKF to produce a noise-optimal and model-robust estimator. The UKF uses statistical linearization and the unscented transformation to replace Jacobian calculations [11], [12]. UKF outperforms EKF in terms of accuracy and reliability. However, it is more computationally intensive as it avoids the EKF's linearization step by using $2n + 1$ sigma points. All the details of implementing UK-SVSF to estimate the PD location can be found in [9].

D. IEKF Formulation

The formulation of the IEKF is described in this section. First, the system's model is reformulated, as shown in the following.

1) Dynamics Reformulation: Let us recall the nonlinear dynamics in (2)

$$\begin{cases} x_t = f(x_{p,t-1}, \omega_t), & \omega \sim \mathcal{N}(0, Q) \\ y_t = h(x_{p,t}, v_t), & v \sim \mathcal{N}(0, R) \end{cases} \tag{11}$$

where

$$\begin{cases} \mathbb{P}\{\omega(0) = 0\} = \mathbb{P}\{v(0) = 1\} = 0 \\ \mathbb{E}[\omega] = \mathbb{E}[v] = 0 \\ \mathbb{E}[\omega\omega^\top] = Q, \quad \mathbb{E}[vv^\top] = R. \end{cases}$$

The fact that (11) follows the Gaussian process allows to reformulate the state equation in the Gaussian process terms as follows [13], [14], [15]:

$$x_{p,t} = \exp(\text{diag}(\text{sign}(\mathcal{F}(x_{p,t-1}))) \, \text{diag}(\psi_t)) \mathcal{F}(x_{p,t-1}) \tag{12}$$

where $\mathcal{F}(\cdot, \cdot) : \mathbb{R}^n \times \mathbb{R}^m \to \mathbb{R}^n$ is a nonlinear function, which expresses the evolution of the system, $\psi \sim \mathcal{N}(0, \overline{Q})$, $\psi \in \mathbb{R}^n$ denotes unknown Gaussian random noise, and the output equation can be reformulated as follows:

$$y_t = \exp(\text{diag}(\text{sign}(\mathcal{H}(x_{p,t}))) \, \text{diag}(\mu_t)) \mathcal{H}(x_{p,t}) \tag{13}$$

where $\mu \sim \mathcal{N}(0, \overline{R})$, $\mu \in \mathbb{R}^q$ denotes unknown Gaussian random noise, $\mathcal{H}(\cdot, \cdot) : \mathbb{R}^n \times \mathbb{R}^m \to \mathbb{R}^q$ is a nonlinear function, which describes the system measured observation, and $y_t \in \mathbb{R}^q$ refers to the system output, which is equal to the measured observation. μ and ψ satisfy

$$\begin{cases} \mathbb{P}\{\psi(0) = 1\} = \mathbb{P}\{\mu(0) = 1\} = 0 \\ \mathbb{E}[\psi] = \mathbb{E}[\mu] = 0 \\ \mathbb{E}[\psi_t \psi_t^\top] = \overline{Q}_t, \quad \mathbb{E}[\mu_t \mu_t^\top] = \overline{R}_t. \end{cases} \tag{14}$$

Remark 1 (Equivalence of Expectation [13], [14]): From (12) to (14), it becomes apparent that $\mathbb{E}[\psi] = \mathbb{E}[\mu] = 0$ implies that $\mathbb{E}[\exp(\text{diag}(\text{sign}(\mathcal{F}(x_{t-1}, u_t)))\text{diag}(\psi_t))]|_{t=1:N} = \mathbf{I}_n$ and $\mathbb{E}[\exp(\text{diag}(\text{sign}(\mathcal{H}(x_t, u_t)))\text{diag}(\mu_t))]|_{t=1:N} = \mathbf{I}_q$, which leaves the system dynamics unaffected in the absence of noise. Thereby, one has

$$\begin{cases} \mathbb{E}[x_t]|_{t=1:N} = \mathbb{E}[\mathcal{F}(x_{t-1}, u_t)]|_{t=1:N} \\ \mathbb{E}[y_t]|_{t=1:N} = \mathbb{E}[\mathcal{H}(x_t, u_t)]|_{t=1:N}. \end{cases} \tag{15}$$

Next, the formulation of the IEKF is derived for discrete-time systems.

2) IEKF Derivation for Discrete Systems: The widely used IEKF is modeled on the Lie group and has been proposed in a geometric matrix form [16]. However, the IEKF [16] framework has not been presented for linear or nonlinear systems in a vector form. Unlike EKF, the IEKF presented in this section mimics the system dynamics presented in (12) and (13). Analogous to EKF, IEKF consists of two stages, namely, propagation and measurement update. Note that for the deterministic part of (12), one has

$$x_{p,t} = \mathcal{F}(x_{p,t-1}) = f(x_{p,t-1}, 0).$$

Hence, the IEKF propagates a priori state estimate utilizing the deterministic part of (12) such that

$$\hat{x}_{p,t|t-1} = f(\hat{x}_{p,t-1}, 0). \tag{16}$$

The error in estimation is defined by

$$\begin{cases} e_{t-1} = x_{p,t-1} - \hat{x}_{p,t-1} \\ e_{t|t-1} = x_{p,t} - \hat{x}_{p,t|t-1}. \end{cases} \tag{17}$$

Thereby, the covariances associated with the error in (17) are given by $P_{t-1} = \mathbb{E}[e_{t-1} e_{t-1}^\top] \in \mathbb{R}^{n \times n}$, $P_{t|t-1} = \mathbb{E}[e_{t|t-1} e_{t|t-1}^\top]$, and $P_t = \mathbb{E}[e_t e_t^\top]$. Similar to (7), using the first-order Taylor series expansion of the nonlinear functions $h(\cdot, \cdot)$ described in (2), one finds

$$\begin{cases} e_{t|t-1} = F_t e_{t-1} + \omega_t \\ y_t - h(\hat{x}_{p,t|t-1}) \approx H_t e_{t|t-1} + v_t \end{cases} \tag{18}$$

where $H_t = (\partial h(\hat{x}_{t|t-1}, 0))/\partial x$, and the high-order terms have been overlooked. P_{t-1} is propagated as follows:

$$P_{t|t-1} = F_t P_{t-1} F_t^\top + Q_t. \tag{19}$$

Fig. 3. Overall system setup. (a) Transformer tank system. (b) Location of the barrier inside the transformer tank model.

Algorithm 2 IEKF Implementation Steps

Initialization:
  1: Set $\hat{x}_{p,0} \in \mathbb{R}^2$ and the covariance $\hat{P}_0 \in \mathbb{R}^{2 \times 2}$
loop
  2: Define H_t, as in (18).
  3: Define $Q_t = \text{Cov}(\omega_t)$ and $R_t = \text{Cov}(v_t)$.
     /* Propagation */
  4: $\hat{x}_{p,t|t-1} = F\,\hat{x}_{p,t-1}$
  5: $P_{t|t-1} = F_t P_{t-1} F_t^\top + Q_t$
     /* Measurement update */
  6: $S_t = H_t P_{t|t-1} H_t^\top + R_t$
  7: $K_t = P_{t|t-1} H_t^\top S_t^{-1}$
  8: $z_t = y_t - h(\hat{x}_{t|t-1})$
  9: $\hat{x}_{p,t} = \exp\big(\text{diag}(\text{sign}(\hat{x}_{p,t|t-1}))\,\text{diag}(K_t z_t)\big)\hat{x}_{p,t|t-1}$
  10: $P_t = (\mathbf{I}_n - K_t H_t) P_{t|t-1}$

end loop

The a priori state estimate in (16) mimics the deterministic part of the true nonlinear measurements in (2). To accommodate for the noise in (12) and mimic the nonlinear dynamics in (12), let us define $z_t = y_t - h(\hat{x}_{p,t|t-1})$ and obtain the a posteriori state estimate as follows:

$$\hat{x}_{p,t} = \exp(\text{diag}(\text{sign}(\hat{x}_{p,t|t-1}))\,\text{diag}(K_t z_t))\hat{x}_{p,t|t-1}. \quad (20)$$

The covariance update is defined by

$$P_t = (\mathbf{I}_n - K_t H_t) P_{t|t-1}. \quad (21)$$

Algorithm 2 summarizes the implementation steps of the IEKF.

E. Noise Uncertainty Mitigation

The filters proposed assume knowledge of the underlying noise statistics plaguing the dynamics and measurement models. The estimation performance will adversely be affected by improper noise covariance magnitude parameters. Consequently, the statistics characterizing the dynamics and measurement sequences is to be identified. For that purpose, we employ an enhanced online MLE routine similar to the one proposed in [8] to aid the filters to stay robust against the aforementioned uncertainties.

The adaptation is given by (22) for the dynamics noise covariance

$$\hat{Q}_{t+1} = K_t e_{t|t-1} e_{t|t-1}^\top K_t \quad (22)$$

and (23) for the measurement noise covariance

$$\hat{R}_{t+1} = e_{t|t-1} e_{t|t-1}^\top - H_t P_{t|t-1} H_t^\top. \quad (23)$$

To improve the numerical stability of the above presented adaptation, a forgetting factor update is used as follows:

$$\hat{Q}_{t+1} = (\alpha)\hat{Q}_t + (1 - \alpha)\hat{Q}_{t+1} \quad (24)$$
$$\hat{R}_{t+1} = (\alpha)\hat{R}_t + (1 - \alpha)\hat{R}_{t+1} \quad (25)$$

where $0 < \alpha < 1$ and its value is empirically set based on observation. In the context of PDL, we recommend a value $\alpha = 0.95$.

The stability characteristics of approaches like the one presented above are addressed in [17].

III. EXPERIMENTAL WORK

A. Setup Description

A sharp point connected to a 40-kV ac supply and immersed inside a tank filled with mineral oil is used to generate the PD at different locations inside the tank. The PD is measured using three AE sensors with a resonance frequency of 45 kHz. The AE sensors are attached to the tank's wall and silicone grease is applied between the tank surface and AE sensors to minimize the reflections on the contact interfaces. The data acquisition equipment used is a 60-MHz bandwidth digital oscilloscope with a sampling rate of 10 million sample/s. The overall system setup is shown in Fig. 3 [2]. Fig. 4 shows the
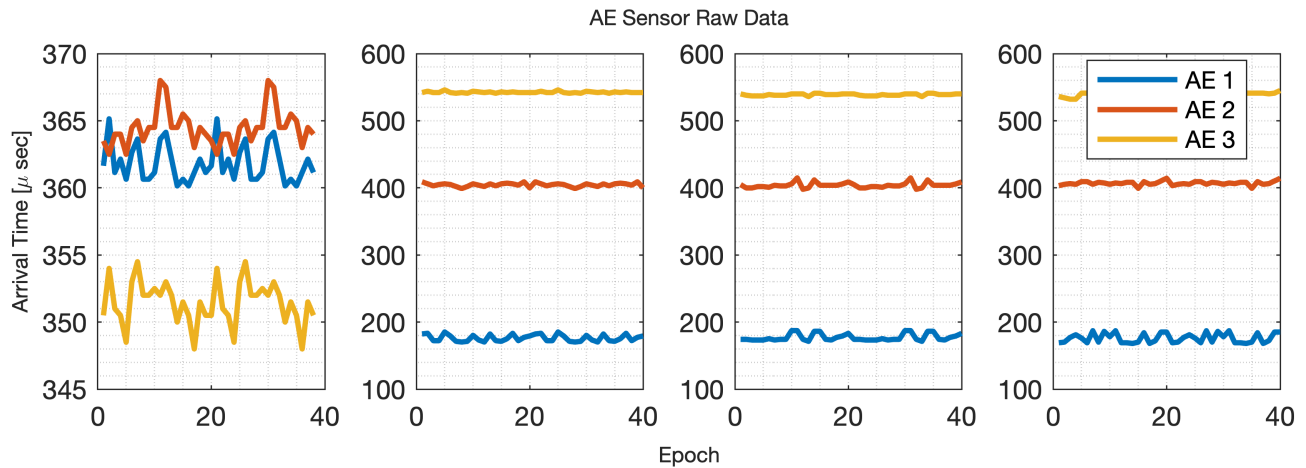
Fig. 4.   Actual measurement of AE PD signals in tests 1–4 from left to right.

measurements from the three AE PD sensors, and the time difference between the AE signals' rising edge of the first wave head and a reference RF signal, where the PD was initiated at location 5 shown in Fig. 2.

B. Experimental Results

This section investigates the IEKF as a computationally simpler alternative for previously proposed stochastic filters for PDL [9]. The effect of varying the initial conditions on the performance of the filters is explored first. For a single experiment, the filters are fed different initial conditions to observe the capacity of each algorithm to recover and converge to the true PD location. Then, the filters are fed data from four experiments to quantitatively describe and evaluate the performance of the proposed IEKF compared to the more traditional filters. A total of four experimental tests are run, and two out of the four experimental runs have added barriers that serve to impede the signals from being detected (see Fig. 5).

C. Effect of Initial Conditions on Estimation Accuracy

The PD location is generally unknown, and initial guesses on its location can be arbitrary. A good estimation algorithm should be able to recover from a bad initialization and not "lock out" or prioritize the dynamics model prediction over the measurement and vice versa. Here, the ability of the proposed IEKF to recover from bad initialization and estimate the PD location is compared against the traditional EKF as well as the hybrid UK-SVSF. The algorithms are evaluated under an array of initial conditions for the chosen experimental test; the filters are run four times equally spaced erroneous initialization. The initial state and initial covariance are set according to Table I in all the test cases. In addition, noise covariance magnitudes of $Q = \mathrm{diag}([2\ 2])$ and $R = 4500$ are used in all the tests.

Fig. 6 presents the experimental results of the chosen test for all the tested conditions. The proposed IEKF is evidently very capable at localizing the PD even when the initial conditions are incorrect. As shown in Fig. 6, the IEKF performs better
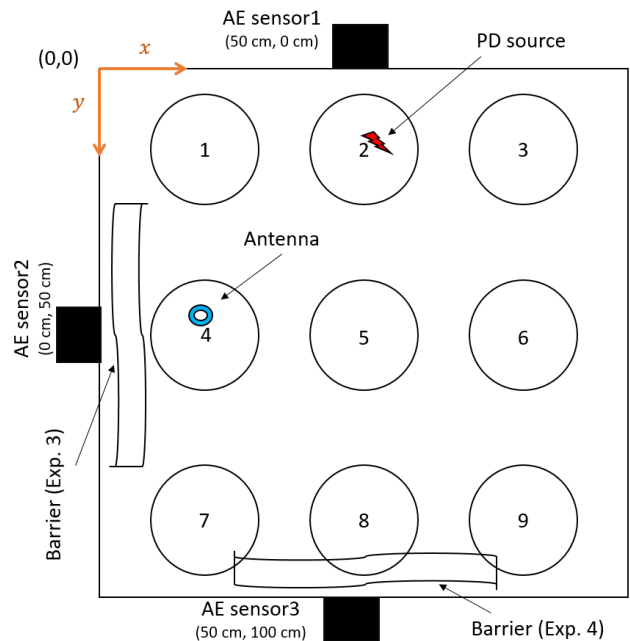

Fig. 5.   Top view of the experimental setup with PD source at location 2 coordinates with barriers installed in front of AE 2 (Experiment 3) and AE3 (Experiment 4).

TABLE I
INITIAL CONDITIONS FOR THE TESTING SCENARIO IN SECTION III-C

Test	$\hat{x}_0\ [cm]$	$P_0\ [cm^2]$
IC_1	$\begin{bmatrix}0.20 & 0.20\end{bmatrix}^\top$	$diag(\begin{bmatrix}60 & 60\end{bmatrix})$
IC_2	$\begin{bmatrix}0.40 & 0.40\end{bmatrix}^\top$	$diag(\begin{bmatrix}60 & 60\end{bmatrix})$
IC_3	$\begin{bmatrix}0.60 & 0.60\end{bmatrix}^\top$	$diag(\begin{bmatrix}60 & 60\end{bmatrix})$
IC_4	$\begin{bmatrix}0.80 & 0.80\end{bmatrix}^\top$	$diag(\begin{bmatrix}60 & 60\end{bmatrix})$

than the traditional EKF in estimating the PD location for every condition tested. The IEKF achieves similar performance to the hybrid UK-SVSF in terms of convergence speed and how close the PD estimate is to the true PD. However, it is noteworthy that the estimate's quality depends on the chosen initial covariance $\hat{P}_0$ corresponding to the certainty
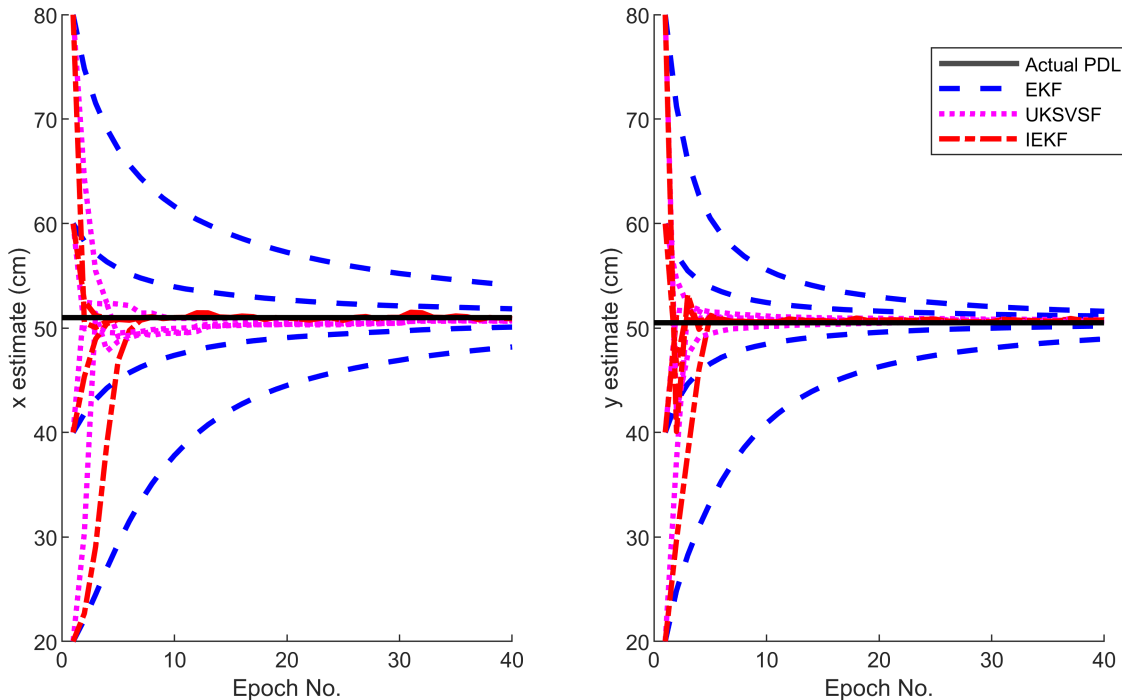
Fig. 6. PDL experimental results.

TABLE II
MONTE CARLO RMSE FOR THE TESTING SCENARIOS

Test	EKF		UKF		SVSF		EK-SVSF		UK-SVSF		IEKF	
	X	Y	X	Y	X	Y	X	Y	X	Y	X	Y
Test 1	1.83	1.00	1.82	1.01	0.16	0.26	0.18	0.33	0.25	0.25	0.16	0.24
Test 2	2.29	2.14	2.20	2.05	0.72	0.29	0.65	0.45	0.69	0.17	0.57	0.19
Test 3	2.23	2.35	2.14	2.26	0.88	0.36	1.02	0.59	0.64	0.23	0.61	0.21
Test 4	2.33	2.27	2.22	2.19	0.57	0.53	0.64	0.68	0.27	0.22	0.28	0.28
Average RMSE	2.17	1.94	2.10	1.88	0.58	0.36	0.58	0.36	0.47	0.22	0.40	0.23
Norm of Averaged RMSE	2.91		2.82		0.68		0.68		0.52		0.46	

of the initial condition being tested as well as the choice of noise covariance magnitude selected when designing the filter. As shown in [18] and [16], the IEKF is immune to the losses in the linearization associated with the classical EKF. This leads to a decreased estimation error with time in the IEKF case, while it might lead to divergence of the EKF. It is evident that the nonlinear structure of the IEKF is proving advantageous to the PDL problem due to the nonlinearities in the system.

D. Algorithm Performance in Different Experimental Tests

Not only is a good estimator able to recover from lousy initialization, but it should also perform well in different conditions and environments. The proposed IEKF is further evaluated on a total of four tests divided into two cases with a barrier covering one of the AE sensors and two cases without.

Fig. 7(a)–(d) shows the comparison between the IEKF, the UKSVSF, and the EKF in localizing PD faults in the four experimental tests performed. Fig. 7(a) and (b) shows the tests without barriers and Fig. 7(c) and (d) shows the tests with barriers. For all the tests, two initial PD locations are assumed and tested. Results back up the finding in Section III-C. The IEKF invariance property shines at estimating the fault location compared with the EKF irrespective of the initial condition, and it performs just as well as the hybrid UKSVSF. Nonetheless, the proposed IEKF is arguably favored here over the UKSVSF given the added complexity with the UKSVSF from both an implementation perspective as well as tuning the various parameters involved to attain good performance.

E. Comparison With Other Methods

It is of interest to also compare the performance of the IEKF in PDL to other stochastic filters. The IEKF is compared with the approaches recently proposed and tested in [9]. The experimental data are processed here based on the IC_2 initialization from Table I. The 100 run-averaged Monte Carlo estimation results in terms of root-mean-square error are presented in Table II. The results indicate that the proposed
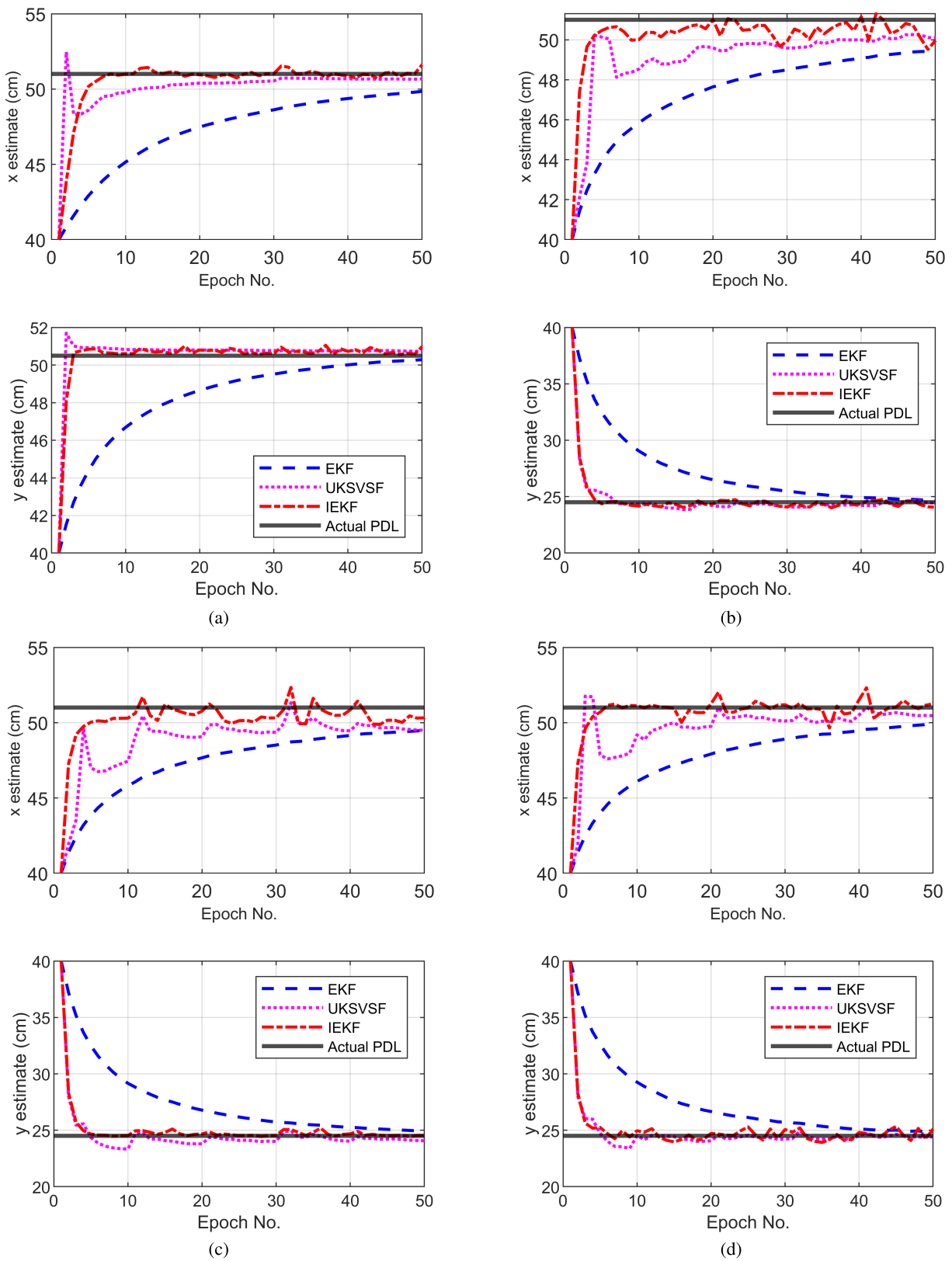
Fig. 7.   Algorithm performance in experimental tests. (a) Test 1 (No barriers). (b) Test 2 (No barriers). (c) Test 3 (Barrier in front of AE 2). (d) Test 4 (Barrier in front of AE 3).

IEKF performs better than traditional approaches such as the EKF and the UKF. Nevertheless, the SVSF method motivated by variable structure theory and sliding mode control contends

with the proposed IEKF and performs similarly. So does hybrid filters derived from the SVSF. However, hybrid filters are reportedly difficult to tune as they involve many more

parameters governing switching between the two filters and parameters affecting each filter's performance.

IV. Conclusion

In this article, a novel IEKF has been proposed to address the problem of PDL. The IEKF is characterized by an invariance property that allows the filter to preserve geometry, preventing error divergence. The filter has been shown to mimic the nonlinear system dynamics in terms of propagation and measurement update.

The IEKF was tested using multiple data sequences involving PD. The discharge was invoked at multiple locations in the experimental tank, and experiments were repeated with and without AE sensor interference in the form of physical barriers installed between the sensor and the tank. Extensive experimental verification of the algorithm established its superiority over the traditional EKF- and UKF-based approaches, especially when the initial conditions fed to the algorithm are incorrect. The IEKF has been successfully implemented at a low sampling rate, revealing the proposed solution's computational inexpensiveness.

Acknowledgment

References

[1] J. Rubio-Serrano, M. V. Rojas-Moreno, J. Posada, J. M. Martínez-Tarifa, G. Robles, and J. A. García-Souto, "Electro-acoustic detection, identification and location of partial discharge sources in oil-paper insulation systems," *IEEE Trans. Dielectr., Electr. Insul.*, vol. 19, no. 5, pp. 1569–1578, Oct. 2012.

[2] R. Hussein, K. B. Shaban, and A. H. El-Hag, "Wavelet transform with histogram-based threshold estimation for online partial discharge signal denoising," *IEEE Trans. Instrum. Meas.*, vol. 64, no. 12, pp. 3601–3614, Dec. 2015.

[3] I. Bua-Nunez, J. E. Posada-Roman, J. Rubio-Serrano, and J. A. Garcia-Souto, "Instrumentation system for location of partial discharges using acoustic detection with piezoelectric transducers and optical fiber sensors," *IEEE Trans. Instrum. Meas.*, vol. 63, no. 5, pp. 1002–1013, May 2014.

[4] R. Ghosh, B. Chatterjee, and S. Dalai, "A method for the localization of partial discharge sources using partial discharge pulse information from acoustic emissions," *IEEE Trans. Dielectr., Electr. Insul.*, vol. 24, no. 1, pp. 237–245, Feb. 2017.

[5] M. Hikita, S. Okabe, H. Murase, and H. Okubo, "Cross-equipment evaluation of partial discharge measurement and diagnosis techniques in electric power apparatus for transmission and distribution," *IEEE Trans. Dielectr., Electr. Insul.*, vol. 15, no. 2, pp. 505–518, Apr. 2008.

[6] W. M. F. Al-Masri, M. F. Abdel-Hafez, and A. H. El-Hag, "A novel bias detection technique for partial discharge localization in oil insulation system," *IEEE Trans. Instrum. Meas.*, vol. 65, no. 2, pp. 448–457, Feb. 2016.

[7] W. M. F. Al-Masri, M. F. Abdel-Hafez, and A. H. El-Hag, "Toward high-accuracy estimation of partial discharge location," *IEEE Trans. Instrum. Meas.*, vol. 65, no. 9, pp. 2145–2153, Sep. 2016.

[8] A. Wadi, W. Al-Masri, W. Siyam, M. F. Abdel-Hafez, and A. H. El-Hag, "Accurate estimation of partial discharge location using maximum likelihood," *IEEE Sensors Lett.*, vol. 2, no. 4, pp. 1–4, Dec. 2018.

[9] M. Avzayesh, M. F. Abdel-Hafez, W. M. F. Al-Masri, M. AlShabi, and A. H. El-Hag, "A hybrid estimation-based technique for partial discharge localization," *IEEE Trans. Instrum. Meas.*, vol. 69, no. 11, pp. 8744–8753, Nov. 2020.

[10] R. F. Stengel, *Optimal Control and Estimation*. North Chelmsford, MA, USA: Courier Corporation, 1994.

[11] E. Wan and R. Van Der Merwe, "The unscented Kalman filter for nonlinear estimation," in *Proc. IEEE Adapt. Syst. Signal Process., Commun., Control Symp.*, Oct. 2000, pp. 153–158.

[12] S. A. Gadsden, S. Habibi, and T. Kirubarajan, "Kalman and smooth variable structure filters for robust estimation," *IEEE Trans. Aerosp. Electron. Syst.*, vol. 50, no. 2, pp. 1038–1050, Apr. 2014.

[13] H. A. Hashim, L. J. Brown, and K. McIsaac, "Nonlinear stochastic attitude filters on the special orthogonal group 3: Ito and Stratonovich," *IEEE Trans. Syst., Man, Cybern., Syst.*, vol. 49, no. 9, pp. 1853–1865, Sep. 2019.

[14] A. H. Jazwinski, *Stochastic Processes and Filtering Theory*. North Chelmsford, MA, USA: Courier Corporation, 2007.

[15] R. Khasminskii, *Stochastic Stability of Differential Equations*, vol. 66. Cham, Switzerland: Springer, 2011.

[16] A. Barrau and S. Bonnabel, "The invariant extended Kalman filter as a stable observer," *IEEE Trans. Autom. Control*, vol. 62, no. 4, pp. 1797–1812, Apr. 2017.

[17] L. Zhang, D. Sidoti, A. Bienkowski, K. R. Pattipati, Y. Bar-Shalom, and D. L. Kleinman, "On the identification of noise covariances and adaptive Kalman filtering: A new look at a 50 year-old problem," *IEEE Access*, vol. 8, pp. 59362–59388, 2020.

[18] A. Barrau and S. Bonnabel, "Invariant Kalman filtering," *Annu. Rev. Control, Robot., Auton. Syst.*, vol. 1, pp. 237–257, May 2018.

Wasim Al-Masri received the B.S. degree in mechanical engineering (minor) in mechatronics from the Jordan University of Science and Technology, Irbid, Jordan, in 2014, and the M.S. degree in mechatronics engineering from the American University of Sharjah, Sharjah, United Arab Emirates, in 2016. He got professional training at the King Abdullah II Design and Development Bureau, Amman, Jordan, in 2013.

He is currently an Instructor with the Department of Mechanical Engineering, American University of Sharjah. His current research interests include sensor fusion, state estimation, control theory, robotics, unmanned aerial vehicles, and mechatronics design.

Ali Wadi (Member, IEEE) received the B.Sc. (cum laude) and M.Sc. degrees in mechanical engineering from the American University of Sharjah, Sharjah, United Arab Emirates, in 2015 and 2017, respectively.

He is currently a Laboratory Instructor with the Department of Mechanical Engineering, American University of Sharjah. His research interests include robotics, modeling, nonlinear dynamics, control systems, drug delivery systems, stochastic estimation, and sensor fusion. He has published over 20 papers in leading refereed journals and conference proceedings.
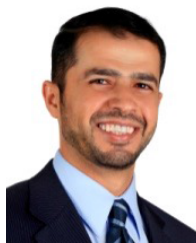
Mamoun F. Abdel-Hafez (Senior Member, IEEE) received the B.S. degree in mechanical engineering from the Jordan University of Science and Technology, Irbid, Jordan, in 1997, the M.S. degree in mechanical engineering from the University of Wisconsin–Milwaukee, Milwaukee, WI, USA, in 1999, and the Ph.D. degree in mechanical engineering from the University of California at Los Angeles (UCLA), Los Angeles, CA, USA, in 2003.

He was a Post-Doctoral Research Associate with the Department of Mechanical and Aerospace Engineering, UCLA, in 2003, where he was involved in a research project on fault-tolerant autonomous multiple aircraft landing. He is currently with the Department of Mechanical Engineering, American University of Sharjah, Sharjah, United Arab Emirates. His research interests are in stochastic estimation, control systems, sensor fusion, and fault detection.

Hashim A. Hashim (Senior Member, IEEE) received the B.Sc. degree in mechatronics from the Department of Mechanical Engineering, Helwan University, Cairo, Egypt, the M.Sc. degree in systems and control engineering from the Department of Systems Engineering, King Fahd University of Petroleum and Minerals, Dhahran, Saudi Arabia, and the Ph.D. degree in robotics and control from the Department of Electrical and Computer Engineering, Western University, London, ON, Canada.

From 2019 to 2021, he was an Assistant Professor with the Department of Engineering and Applied Science, Thompson Rivers University, Kamloops, BC, Canada. He is currently an Assistant Professor with the Department of Mechanical and Aerospace Engineering, Carleton University, Ottawa, ON, Canada. His current research interests include vision-based aided navigation and control, localization and mapping, stochastic and deterministic estimation, sensor fusion, and distributed control of multiagent systems.

Ayman H. El-Hag (Senior Member, IEEE) received the B.S. and M.S. degrees from the King Fahd University of Petroleum and Minerals, Dhahran, Saudi Arabia, in 1993 and 1998, respectively, and the Ph.D. degree from the University of Waterloo, Waterloo, ON, Canada, in 2003.

He joined Saudi Transformer Company, Dammam, Saudi Arabia, as a Quality Control Engineer from 1993 to 1999. From January to June 2004, he worked as a Post-Doctoral Fellow with the University of Waterloo. He was with the University of Toronto, Toronto, ON, Canada, as an NSERC Post-Doctoral Fellow from July 2004 to July 2006. In 2006, he joined the Department of Electrical Engineering, American University of Sharjah, Sharjah, United Arab Emirates, where he was promoted to an Associate Professor and then to a Professor in 2011 and 2016, respectively. He is currently a Lecturer at the Department of Electrical and Computer Engineering, University of Waterloo. His current main areas of interest are condition monitoring and diagnostics of electrical insulation and application of machine learning in power engineering.

Dr. El-Hag was the Middle East Editor of the IEEE ELECTRICAL INSULATION MAGAZINE from 2016 to 2018. He is also an Associate Editor of the IEEE TRANSACTIONS ON DIELECTRIC AND ELECTRICAL INSULATION and a member of the IEEE Outdoor Insulation Committee. He was a member in the IEEE Std 1523 (IEEE Guide for the Application, Maintenance, and Evaluation of Room Temperature Vulcanizing (RTV) Silicone Rubber Coatings for Outdoor Insulation Applications) and IEEE Standard 2652, "IEEE Guide for DC Inclined Plane Tracking and Erosion Test for Outdoor Insulation Applications."